Sensors & Diagnostics

CRITICAL REVIEW
Neso Sojic *et al.*
Recent advances in electrochemiluminescence
immunosensing

Check for updates

Recent advances in electrochemiluminescence immunosensing

Jing Yu,[a] Dalibor Stankovic, [iD][b] Jasmina Vidic[c] and Neso Sojic [iD] *[ad]

Electrogenerated chemiluminescence, also called electrochemiluminescence (ECL), has attracted much attention in various fields of analysis due to its high sensitivity, extremely wide and dynamic range and excellent control of space and time of the light emission. The great success of ECL for *in vitro* detection results from the advantages of combining the selectivity of biological recognition elements and the sensitivity and controllability of ECL technology. ECL is widely applied as a powerful analytical technique for ultrasensitive detection of biomolecules. In this review, we summarize the recent developments and applications of ECL for immunosensing. Herein, we present the sensing schemes and their applications in different areas, such as detection of biomarkers, bead-based detection and bacteria and cell analysis and provide future perspectives on new developments in ECL immunosensing. In particular, ECL-based sensing assays for clinical sample analysis and medical diagnostics and the development of immunosensors for these purposes are highlighted.

1. Introduction

Electrochemiluminescence (ECL) is a chemiluminescence (CL) phenomenon triggered by an initial electrochemical process.[1–4] Compared to conventional CL, it exhibits several advantages resulting from the use of electrochemical methods, including simplicity, stability and ease of use. In addition, ECL has superior temporal and spatial control on light emission. Also, the absence of excitation light in ECL promises a near-zero background, while fluorescence or phosphorescence suffers from an unselective photoexcitation-inducing background. Since the first ECL studies were published in the mid-1960s,[5,6] extensive research efforts have been pouring into the ECL field, and now ECL is a well-established powerful analytical technique and widely used in many applications, such as ECL imaging,[7,8] bioanalysis,[9–11] DNA probe assays,[12] food safety analysis[13] and environmental monitoring.[14]

A paramount breakthrough in the development of ECL is the ECL immunoassay, which combines the specific immunoreaction with the intrinsic properties of ECL, enabling the sensitive and specific detection of targets with a fast analysis procedure and simple device. It has been applied commonly in the analysis of trace immunogenic substances, showing the characteristics of good specificity, high sensitivity and selectivity, short time consumption and high trace determination. The working principle of the ECL immunosensor is similar to that of the traditional immunoassay; the antigen or antibody is generally functionalized by ECL luminophores and immobilized on the electrode surface, and the specific recognition of antigens or antibodies can then cause changes in ECL response signal, thereby achieving the detection with quantitative analysis of the target protein and high efficiency of the sample. ECL-based immunoassays are commercialized for clinical diagnostics mainly by two companies (Roche Diagnostics and Meso Scale Discovery), with ≈2 billion assays running worldwide per year.[15,16] This review highlights the recent developments in ECL immunosensing, such as new detection schemes, detection of protein biomarkers, bacteria analysis, cell analysis and other bioanalytical applications. Lastly, future prospects for the development of ECL immunosensor has been discussed.

2. Fundamentals of ECL

2.1. ECL mechanisms

Generally, ECL can be generated by either the annihilation pathway or the co-reactant pathway. In the annihilation pathway, radical anion and cation of the luminophore are firstly electrogenerated on the cathode and anode, respectively, or by pulsing the same electrode at sufficient cathodic and anodic potentials. Then, anion and cation react exergonically with each other to generate the excited state of

[a] *College of Chemistry and Chemical Engineering, Yantai University, Yantai 264005, China*
[b] *Faculty of Chemistry, University of Belgrade, Studentski trg 12-16, 11000 Belgrade, Serbia*
[c] *INRAE, AgroParisTech, Micalis Institute, UMR 1319, Université Paris-Saclay, 78350 Jouy-en-Josas, France*
[d] *University of Bordeaux, CNRS, Bordeaux INP, Institut des Sciences Moléculaires, UMR 5255, 33607 Pessac, France. E-mail: sojic@u-bordeaux.fr*

the luminophore. It relaxes to the ground state, followed by light emission. However, this pathway is usually performed in organic solvents because it requires usually quite negative and positive potentials. Meanwhile, in the co-reactant pathway, the luminophore and co-reactant can be electrochemically oxidized or reduced on the electrode surface by pulsing a positive or negative unidirectional step potential. The electrogenerated intermediates undergo homogeneous electron-transfer reactions to form the excited state luminophore, which can relax to the ground state with light emission. The co-reactant pathway is most largely used in analytical and bioanalytical applications because ECL is generated in aqueous media at physiological pH values.[3,10,17,18]

2.2. The ECL emitters

The archetypal ECL luminophores are tri(2,2′-bipyridine) ruthenium(II) ([Ru(bpy)$_3$]$^{2+}$) and luminol.[4,8,12,19] Afterward, the pursuit of ECL luminophores with higher ECL efficiency and lower excitation potential has pushed the exploration of new organometallic complexes, mainly based on iridium, and of nanomaterials. The model ECL system composed of the [Ru(bpy)$_3$]$^{2+}$ luminophore and tri-n-propylamine (TPrA) co-reactant has achieved overwhelming success for immunosensing, because of high sensitivity, specific chemical reactivity, extremely wide dynamic range, rapidness, simplicity and excellent controllability.[20] Secondly, other metal complexes, such as transition metal complexes incorporating Ru, Os and rare earth chelates, including Ir, Au and Pt, have been reported as ECL labels enabling color tuning for light-emitting systems.[1] Luminol and its analogues (e.g. 8-amino-5-chloro-2,3-dihydro-7-phenyl-pyrido[3,4-d] pyridazine-1,4-dione, L-012) operating with H$_2$O$_2$ constitutes a popular system that is widely used to generate ECL, due to its low cost, low oxidation potentials, easy functionalization and broad bioanalytical applications.[21] Finally, nanomaterials, including nanoparticles, porous luminophore-doped nanoparticles, quantum dots (QDs), carbon-based materials, metal composites and even aromatic hydrocarbon nanoparticles have been used in ECL sensing and imaging.[22,23] Luminophore-doped silica nanoparticles have also been developed with remarkable performances for efficient ECL emission.[24–27] After the initial silicon QDs (Si semiconductor) reported in 2002,[28] many QD-based ECL emitters, II–VI, III–V and IV–VI nanocrystals, carbon QDs with different sizes, shapes and compositions have generated great interest for their potential ECL applications on account of their size-controlled photoluminescence and excellent stability against photobleaching. Up to now, a series of III–V and II–VI QDs, such as CdSe, CdTe, PbS, CdS and carbon-based materials, such as carbon dots (CDs), graphene quantum dots (GQDs) and graphene-like C$_3$N$_4$ nanosheets (g-C$_3$N$_4$ NSs) have been exploited as promising ECL nanoemitters.[29,30] Significantly, nanoclusters (NCs) or nanoparticles (NPs), particularly, noble metal NCs/NPs, are often introduced into ECL system as labels

to improve ECL efficiency, due to their ultra-small size and nontoxicity. For example, Au$_{18}$, Au$_{21}$, Au$_{25}$, and Au$_{38}$ NCs have appeared, enriching the type of Au NCs and providing new insights into ECL applications.[31,32] In addition to the various sizes of Au NCs, their various valence states are found to be important for ECL biosensing applications, especially in the near-infrared region.[33–36] In this review, we will summarize the studies related to ECL immunosensing with the emitters mentioned above.

3. Analytical applications and strategies

3.1. Bead-based ECL immunoassays

Bead-based ECL assays have been the object of numerous works and are commercialized for the quantification of a large number of biomarkers involved in various pathology studies, such as cardiac and infectious diseases, thyroid and tumor markers, bacteria, and viruses.[37–39] Generally, in such assays, magnetic beads with micrometric sizes are functionalized with a specific capture antibody. In the sandwich format, the biorecognition chain is continued with the analytical target (e.g. the antigen), if present in the sample, and a detection antibody is labeled with the ECL luminophore. Classically, [Ru(bpy)$_3$]$^{2+}$ is used as the label and the co-reactant is the freely-diffusing TPrA. ECL of this efficient ECL system is combined with magnetic beads in a flow cell because it offers several advantages in automated immunoassays for the quantification of biomarkers in body fluids: (i) the 3D structure of the beads increases the surface-to-volume ratio, (ii) easy preprocessing and processing of the samples during separation, enrichment, and washing steps, (iii) the application of an external magnetic field captures the magnetic beads carrying the labeled immuno-complexes on the working electrode, (iv) the precise control over time and position generates the analytical ECL signal in front of the photodetector.[16] The capture of the bead on the electrode surface is an essential step because ECL is a surface-confined technique. In other words, the beads carrying the immuno-complexes with the ECL labels have to be very close to the electrode surface where the co-reactant radicals are produced electrochemically due to their limited lifetimes.[20,40] The reactivity of the TPrA radicals governs mainly the sensitivity of the assay. The spatial distribution of ECL emission at the surface of the bead can be mapped by employing ECL microscopy (Fig. 1). Several groups investigated the mechanisms operating in such assays by imaging the spatial distribution on beads.[40–46] Initially, they reported the ECL detection of streptavidin-modified [Ru(bpy)$_3$]$^{2+}$-label with TPrA or DBAE in a top-view or side-view configuration, this 3D imaging approach provides insights into the ECL mechanistic route operating in bioassays and on the optical effects.[40] Later, the dynamic imaging of the ECL reactivity in space at the single-bead level was further studied to investigate the kinetics of the [Ru(bpy)$_3$]$^{2+}$/TPrA system.[42] Then, the optical effects due to the light propagation through
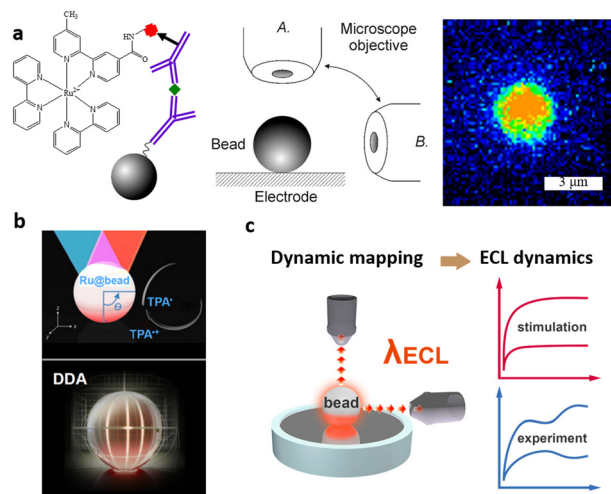
Fig. 1 a) Schematic of bead-based ECL imaging in top (A) and side-view (B) configurations.[40] b) Simulations of the optical effects by DDA.[44] c) Dynamic imaging at the single bead level.[42] Reprinted with permission from ref. 40 (copyright 2014 Royal Society of Chemistry), ref. 42 (copyright 2023 American Chemical Society), ref. 44 (copyright 2023 American Chemical Society).

the bead decorated with the ruthenium labels were reported,[44] determining mainly the spatial distribution of the recorded 3D ECL signals. The combination of ECL microscopy and optical modelling based on the discrete dipole approximation (DDA) provided global description of the ECL chemical reactivity and the possibility of investigating the chemical mechanism by deconvoluting the ECL patterns from the optics. The factors influencing the kinetics of ECL were found, which could support the optimization of ECL immunoassays.

Many strategies were implemented to enhance ECL signals for bead-based immunoassays.[41] For example, Paolucci and coworkers reported the insertion of carbon nanotubes to extend and enhance the ECL emission.[47] It leads to a remarkable enhancement of the ECL intensity by increasing the efficiency of the "remote" ECL mechanism and the concurrence of an additional ECL-generating mechanism. To extend the ECL-emitting layer, Dai and coworkers demonstrated the use of conductive gold beads.[48] In comparison with non-conductive magnetic beads, they obtained a 21.7-fold increase in the turn-over frequency of ECL generation with such gold beads. In addition, in this case, the ECL generation is no longer restricted by the limited lifetime of the electrogenerated TPrA radicals. Finally, the authors reported the development of size-encoded multiplex assays for the simultaneous detection of four kinds of acute myocardial infarction biomarkers, namely, CRP, cardiac troponin I (cTnI), fatty acid-binding protein, and myoglobin. Qi and coworkers also played with the electrode design by developing a gold nanoelectrode ensembles[49,50] taken as a disposable ECL platform with immunomagnetic beads.[51] Since the electrode material is an essential parameter in ECL,[52–56] various materials were tested. For example, Einaga and coworkers exploited boron-doped

diamond as an electrode material for ECL immunoassay based on the $[Ru(bpy)_3]^{2+}$/TPrA system and compared it with the approach used in commercial instrumentation (*i.e.* Pt).[57] They obtained an increase of 70% in the resulting ECL and a double signal-to-noise ratio compared to Pt electrodes. The same group reported an original strategy based on the *in situ* electrochemical generation of H_2O_2 at a boron-doped diamond electrode. Hydrogen peroxide reacted with the beads labeled with luminol that were deposited on the electrode surface.[58] However, the main drawback is that luminol is a sacrificial luminophore that can generate a photon just once per molecule whereas $[Ru(bpy)_3]^{2+}$ is regenerated during the ECL reaction and generates several photons in the presence of a sacrificial co-reactant.

The composition of the solution was also investigated to improve the performances of bead-based assays. Various surfactants have been added to increase (i) the efficiency of the TPrA oxidation since it is a key step to promote ECL emission[59,60] and (ii) the solubility of TPrA. Valenti and coworkers exploited the buffer capacity of the solution to modify the rate of the reactions involved in the ECL generation. They demonstrated a "chemical lens effect" that enabled modification of the thickness of the ECL-emitting layer at the bead level.[61] Moreover, the same group was able to increase ECL emission by a maximum of 128% through (i) optimization of luminophore distribution by decreasing the bead size and (ii) addition of a branched amine to increase the efficiency of the co-reactant mechanism.[20] They reported a highly efficient mechanistic path for ECL generation, very close to the electrode surface. This highlights the importance of investigating the ECL mechanism and the optical effects occurring in the bead-based assays.[42,44,62] Francis and coworkers proposed a very original possibility by adding a redox mediator that can act as both an electrocatalyst for TPrA oxidation and a more stable alternative to TPrA$^{·+}$ for the chemi-excitation of the luminophore.[7,63,64] They tested several water-soluble Ir(III) complexes[43] as redox mediators and found that $[Ir(sppy)_3]^{3-}$ (where sppy = 5′-sulfo-2-phenylpyridinato-C^2,N) elicited a significant improvement (70.9-fold at 0.9 V and 2.9-fold at 1.2 V) of the ECL signal from $[Ru(bpy)_3]^{2+}$ labels immobilized on the surface of the beads. It is due to the combination of (i) high solubility in aqueous solution, (ii) a chemically and electrochemically reversible oxidation (E_{ox}) at a potential close to that of the irreversible oxidation of TPrA, (iii) an E_{red} beyond the reduction strength of TPrA$^·$, and (iv) a greater excited state energy than $[Ru(bpy)_3]^{2+}$. However, the Ir(III) complexes also generated ECL light. Therefore, the same group prepared a non-emissive sulfonated tris(1-phenylpyrazolato)-iridium(III) ($[Ir(sppz)_3]^{3-}$) that is an effective enhancer of the ECL reaction of $[Ru(bpy)_3]^{2+}$ and TPrA in aqueous solution, without an inherent interfering emission.[65] They showed the potential application of this approach for the development of highly efficient redox-mediated ECL for ultrasensitive biomarker detection and for practical sample analysis.

New Ir(III) complexes acting as ECL luminophores (and not redox mediators as described in the previous paragraph) were designed to improve ECL efficiency for immunosensing and also the multiplexing.[53–56] The $[Ru(bpy)_3]^{2+}$-grafted microgels with 3D network (diameter ~100 nm) were used to decorate micrometric beads, enhancing ECL signals.[66] The fraction of $[Ru(bpy)_3]^{2+}$ centers located on the very bottom of the microgels can let them oxidize directly at the GCE surface and react with TPrA efficiently. Thus, stable and efficient ECL emission was obtained. Moreover, a new kind of co-reactant BIS-TRIS can be also introduced into a bead-based ECL system to well balance ECL distance reactivity trade-off and enhance the sensitivity by 236% compared with TPrA for the detection of carcinoembryonic antigen.[45]

Feng and coworkers followed a different strategy by imaging single molecules at single-photon sensitivity using ECL.[67] They applied their detection scheme to single-molecule ECL bioassay in order to detect carcinoembryonic antigen, showing a limit of detection of 67 attomoles, a concentration 10 000 times better than that from conventional ECL bioassays.[68]

3.2. ECL immunosensors for protein biomarker detection

As a subcategory of biomarkers, protein biomarkers have become hot target analytes in ECL immunoassay.[69] Protein biomarkers are a kind of substances that are secreted in the process of disease occurrence and even deterioration, or abnormal changes of the body in response to diseases, which reflect the existence and process of diseases, and are recognized as reliable dynamic indexes to diagnose diseases. In some points, protein biomarkers can be classified into three types, enzymes, hormones and other proteins. The common protein biomarkers related to the tumor, include carcinoembryonic antigen (CEA), carbohydrate antigen (CA), alpha fetoprotein, prostate-specific antigen (PSA) and mucin 1 (MUC1). The other proteins, such as cTnI, C-reactive protein (CRP), lactoferrin, β2-microglobulin, are the biomarkers for the detection of other diseases. Here, we summarize the ECL immunosensing for detecting disease biomarkers.

3.2.1. ECL immunosensors for tumor biomarker detection.
Various ECL immunosensing systems,[50,70–72] such as sandwich-type ECL immunosensors, competitive ECL immunosensors, and even ECL aptasensors, have been developed for the detection of protein biomarkers, shown in Fig. 2. As a glycoprotein produced by the yolk sac and embryonic liver, AFP has become the most sensitive biomarker of primary liver cancer. Yuan and co-authors[73] reported a direct detection of α-1-fetoprotein (AFP) on Au NPs modified glassy carbon electrode (GCE) developed by using $[Ru(bpy)_3]^{2+}$-doped silica/Au (Ru-silica@Au) composite as labels.

Ju and co-authors[74] designed a competitive immunosensor by using Au NPs coupled with polyaniline as an energy receptor to absorb energy emitted from polyoxomolybdate–
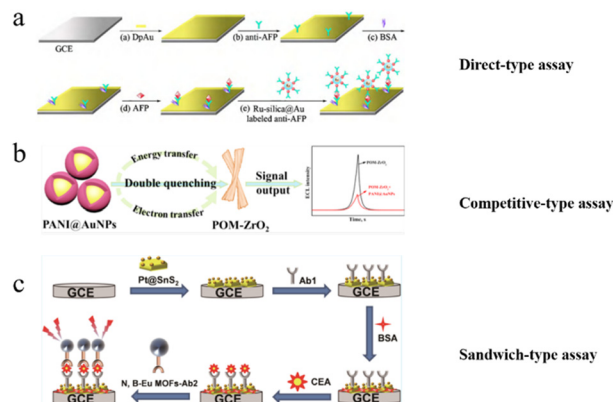

Fig. 2 Schematic of three kinds of ECL immunosensing system. a) Direct-type ECL assay for the detection of AFP.[73] b) Competitive-type ECL assay for the detection of AFP.[74] c) Sandwich-type ECL assay for the detection of CEA.[75] Reprinted with permission from ref. 73 (copyright 2010 Elsevier), ref. 74 (copyright 2022 American Chemical Society), and ref. 75 (copyright 2022 American Chemical Society).

ZrO_2 (energy donor). The energy and electron transfer occurred at the same time for quenching the ECL intensity of polyoxomolybdate–ZrO_2. This dual-mechanism quenching strategy was applied to detect 17β-estradiol. CEA is considered to be one of the tumor markers for the clinical diagnosis of various tumors, such as lung cancer, breast cancer, and colorectal cancer. Yang and co-authors[75] proposed a sandwich-type immunosensor by using $Pt@SnS_2$ as a matrix and N, B-doped Eu MOF (N, B-Eu MOF) nanospheres as a signal amplifier for highly sensitive and selective detection of CEA. The dual "antenna" effect of 5-boronoisophthalic acid (5-bop) and 5-nitroisophthalic acid (5-nop) enabled the N, B-Eu MOFs to show a very good ECL signal. Thus, this sandwich-type immunosensor provided specific immune responses for the detection of CEA. Deng et al.[76] established a co-reactant-dependent ratiometric ECL sandwich-type immunosensor by using ZnSe@ZnS QD conjugated with poly-(diallyldimethylammonium chloride) (PDDA) reduced graphene oxide (PDDA-rGO) and second antibody to detect CEA in human serum. Furthermore, red-emitting (680 nm) carbon QDs (RCQDs) as luminophores were introduced to construct sandwich-type ECL immunosensors for the detection of CEA.[77] The secondary antibody label fabricated by the synthesis of aminated graphene can remarkably quench the ECL of RCQDs modified on the electrode because of the ECL resonance energy transfer; thus, this immunological recognition sensitively quantifies CEA through ECL quenching.

CA is identified from tumor cell lines by monoclonal antibody technology, so it exhibits high accuracy in the diagnosis of specific tumors. Different types of CAs, such as CA125,[78] CA153 (ref. 79) and CA 199,[51] have been chosen as the model analytes for ECL bioassays, among which CA125 is the primarily used diagnostic biomarker for epithelial ovarian cancer and endometrial cancer. CA153 and CA199 are specific to breast and pancreatic cancers, respectively. A sandwich-

type ECL immunosensor was proposed for the sensitive detection of CA 125 on a nanoporous gold (NPG) modified GCE. $[Ru(bpy)_3]^{2+}$–gold nanoparticles (Ru–AuNPs) composite assembled with poly(diallyldimethylammonium chloride) functionalized graphene nanosheets (GR) (Ru–AuNPs/GR) was used as ECL labels, modified on the electrode. This proposed sandwich-type ECL immunocomplex provide a wide linear response range over 0.01–100 U mL^{-1} with a detection limit of 0.005 U mL^{-1}.[78] Yang et al.[51] proposed a disposable ECL immunosensor for CA199 detection with a special Au nanoelectrode as the platform, magnetic bead as the capture probe, and $[Ru(bpy)_3]^{2+}$-labeled antibody as the ECL indicator, which brought hopes for the detection of biomarkers at the point-of-care test.

PSA, an oncofetal glycoprotein, is a widely used tumor marker, which is expressed in normal mucosal cells and overexpressed in prostate cancer. Xu et al.[80] proposed a dual ECL enhancement strategy on a closed ITO bipolar electrode for PSA detection in human serum. Au NPs catalyzed the anodic ECL reaction between luminol and H_2O_2, meanwhile, thionine (Th)@SiO$_2$ NPs were introduced in cathodic pole as the recognition probes of PSA and signal amplification indicators. By using various QDs as ECL indicators, Fu et al.[81] prepared several sandwich-type ECL immunosensors for PSA detection with a wide detection range, presenting promising application potential in clinical diagnosis. Currently, the label-free detection technique is a new kind of detection strategy without the usage of labels, attracting much attention. It is based on the direct detection of changes in physical parameters, such as impedance, capacitance, optical properties, or mass change during antigen and antibody interactions without the secondary antibody. Liu et al.[82] reported a strategy quantified by the ratio of cathodic and anodic signals (ECL$_{cathodic}$/ECL$_{anodic}$) to determine PSA in human serum. The measured PSAs were immobilized on the CdS QDs electrode to generate a cathodic working signal and the fixed PSA was modified on the luminol–Au NPs electrode to get the anodic signal. This ECL immunosensor offers reliability for detecting PSA through simple tests.

3.2.2. ECL immunosensors for other disease biomarker detection. Tumor biomarker detections by ECL sensing were mentioned above, but with the acceleration of the aging process among the global population, other diseases, such as

heart disease, and Alzheimer's disease, are continuously troubling the elderly. Hence, it is imperative to develop sensitive and specific ECL sensing platforms for the detection of other disease biomarkers.

cTnI is considered the golden standard for myocardial infarction screening. An ECL immunosensor fabricated using luminol–AuNPs as both antibody carriers and sensing platform was described for the detection of myocardial infarction biomarker cTnI in clinical diagnosis, as shown in Fig. 3.[83] Xu et al.[84] proposed a visual and high-throughput ECL immunosensor with a simple-electrode system, achieving the simple but accurate determination of cTnI via employing the smartphone as the detector. CRP, as the sensitive indicator of infection and inflammation, is also a general biomarker to evaluate a patient's risk for AMI and cardiovascular diseases. Recently, the first lateral flow-based ECL immunosensor was established via the co-reactant pathway. A sandwich immunocomplex generated strong ECL emission with the $[Ru(bpy)_3]^{2+}$/TPrA system, allowing full-range CRP detection with high sensitivity due to the simple detection device and easy operation procedure.[85] A simple and effective ECL immunosensor for quantitative detection of CRP was reported on the modified ITO electrode.[86] The ITO was prefunctionalized by Ti NTs and Pt NWs and with Nafion as a linker, the CRP antibody was then attached and finally this sensor was constructed by blocking the residual active sites with BSA. The introduction of nano-composite significantly promoted the sensing performance for CRP assay.

Alzheimer's disease (AD) is actually a brain disease that seriously influences the daily life of the elderly. It is crucial to develop sensitive and specific ECL immunoassays to realize the early intervention of AD by detecting its corresponding biomarkers. β-Amyloid$_{1-42}$ (Aβ$_{42}$) oligomers with strong neurotoxicity are considered well-established and internationally validated model analytes for early diagnosis of AD. Liu et al.[87] presented a simple signal-on ECL aptasensor by using the co-reactant mechanism for the detection of amyloid-beta (Aβ) peptide. ROS as a co-reactant was generated via a catalysis reaction between Cu^{2+}-Aβ. It reacted with luminol to exhibit favorable analytical performance for the Aβ16 monomer with a low detection limit of 3.5×10^{-14} mol L^{-1}. Tu et al.[88] recently proposed a dual-screening ECL bioassay by employing mesoporous silica membrane as the nano-sieving and specific aptamer as the capturer, which achieved the discrimination of the Aβ monomer from the Aβ oligomer and fiber, and offered a promising opportunity to detect Aβ in complex matrices.

Human epididymis protein 4 (HE4) is a specific biomarker for ovarian cancer. An enhanced ECL immunosensor was designed based on an efficient TiO$_2$ MCs@rGO loading with luminol/DBAE system for amplifying ECL emission, realizing the quantitative analysis of HE4.[89] An ECL signal amplification strategy was proposed via employing carbon nano-horns as the photothermal converter to elevate the electrode surface temperature, and a ratiometric ECL immunosensor exhibited excellent sensitivity for HE4 detection.[90]
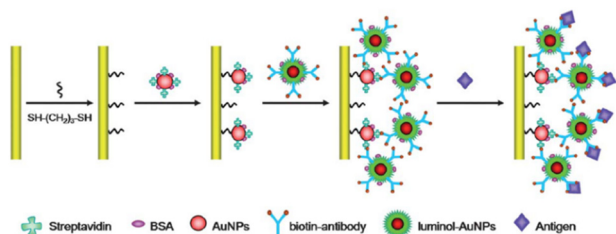

Fig. 3 Schematic of the fabrication processes of the ECL immunosensor fabricated using luminol–AuNPs as antibody carriers and sensing platform.[83] Reprinted with permission from ref. 83 (copyright 2013 Royal Society of Chemistry).

3.2.3. ECL immunosensors for other protein detection. In addition to the above protein biomarkers used for tumor or common disease diagnosis, some other kinds of proteins have also been involved in ECL immunoassays, such as human IgG, hormone-based biomarkers and enzyme-based biomarkers.

Ju and co-authors[91] reported a competitive immunosensor constructed by immobilizing *meso*-2,3-dimercaptosuccinic acid (DMSA)-stabilized CdTe QDs and human IgG (HIgG) as antigen on GCE, shown in Fig. 4. The competitive immuno-recognition of the immobilized HIgG and analyte HIgG to horseradish peroxidase (HRP)-labeled antibody produce on a HRP-immobilized surface, leading to the detection of HIgG with high sensitivity. CdS QDs-carbon nanotubes (CNTs) and Au NPs–chitosan as effective antibody immobilization matrix were presented to detect the target human IgG.[92]

A sandwich ECL immunosensing platform based on bifunctional polymer dots (TEA–Tyr dots) and reduced graphene mesoporous silica gold hybrids was designed for ultrasensitive detect cytokine biomarker (IL-6), realizing the quantitative and qualitative dual signal amplification (Fig. 5). The two synergistic effects between TEA and the tyramine group (Tyr) improved the sensitivity remarkably.[93] Hormone-based biomarkers and enzyme-based biomarkers have become promising model targets for ECL bioassays. At present, the most frequently investigated hormone-based biomarkers in ECL immunoassays are many kinds, including insulin,[94] thyroid stimulating hormone (TSH),[95] procalcitonin (PCT)[96] and human chorionic gonadotrophin (HCG).[97] Insulin is the target analyte for diabetic mellitus, TSH is related to hyperthyroidism, PCT is an indicator of inflammation, and HCG is a biomarker of pregnancy. As for enzyme-based biomarkers, thrombin,[98] protein kinase A (PKA),[99] *N*-acetyl-β-D-glucosaminidase,[100] and apurinic/apyr-imidinic endonuclease 1 (ref. 101) have been widely applied as the target analytes in the construction of ECL biosensing methods.

3.3. ECL immunosensors for bacterial analysis

Pathogenic bacteria pose a significant threat to human health and safety, highlighting the critical need for early detection methods. Rapid detection of pathogens in the initial stages
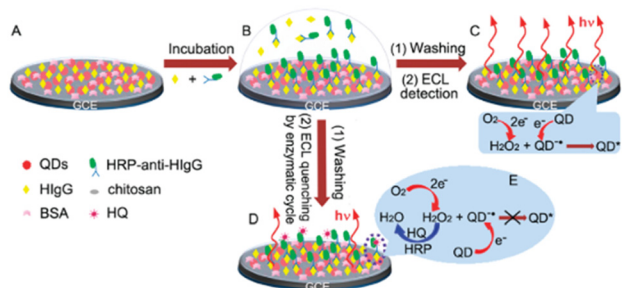
Fig. 4 Construction (A) and incubation (B) of the immunosensor, and ECL detection without (C) and with (D and E) the enzymatic amplification by consumption of H_2O_2 as co-reactant.[91] Reprinted with permission from ref. 91 (copyright 2010 American Chemical Society).
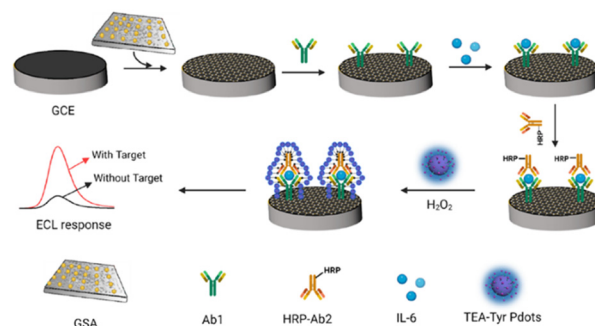
Fig. 5 The fabrication process of sandwich ECL immunosensor based on bifunctional P dots (TEA–Tyr dots).[93] Reprinted with permission from ref. 93 (copyright 2022 American Chemical Society).

of infection is crucial for selecting appropriate treatment, suppressing pathogen transmission, reducing mortality rates, and minimizing economic burden. While conventional techniques such as polymerase chain reaction and enzyme-linked immunosorbent assays are accurate, their complexity and time-intensive nature often hinder widespread applications. ECL immunosensors offer a promising solution by combining the advantages of both electrochemical and photoluminescence analyses, enabling highly sensitive and simple detection of pathogenic bacteria. In this section, we will address the latest developments in ECL sensors for the detection of pathogenic bacteria.

In the work of Wei and co-authors,[102] a newly developed dual-mode detection ECL/SERS immunosensor offers a precise method to quantify pathogenic *Vibrio vulnificus*. This Gram-negative bacterium is widely distributed in seawater and seafood, and there is a need for its sensitive and rapid on-site detection. The biosensor was based on a multifunctional 2D $Ti_3C_2T_x$ MXene loaded with ECL signal tags ABEI and detection of Ab_2 antibodies. Due to numerous surface functional groups of $Ti_3C_2T_x$ MXene it was also loaded with SERS signal tags rhodamine 6G and closely packed plasmonic gold nanorods to enable SERS measurements. The utilisation of 2-D MXene for electrode functionalization thus allowed the construction of a dual-mode immunosensor with improved sensitivity and accuracy. Under optimal experimental conditions, *Vibrio vulnificus* was detected with the limit of quantification for ECL and SERS of 1 CFU mL^{-1} and 10^2 CFU mL^{-1}, respectively.

Similarly, the advantages of MOFs were exploited to construct an ECL immunobiosensor for *Burkholderia pseudomallei* detection.[103] A new type of versatile catalytic nanomaterial called Co-MOF@AuNP@ABEI has been introduced, comprising cobalt-doped metal–organic frameworks (Co-MOF), gold nanoparticles (AuNP), and *N*-(4-aminobutyl)-*N*-(ethylisoluminol) (ABEI). This nanomaterial demonstrates remarkable catalytic properties, displaying high synergistic effects and zero-distance catalysis, which significantly enhances the sensitivity of an ECL biosensor. By integrating with the ECL system and a 3D magnetic walking nanomachine amplification approach, the Co-

MOF@AuNP@ABEI achieved an exceptionally sensitive ECL assay for *Burkholderia pseudomallei*, with a detection limit of as low as 60.3 aM. This LOD surpasses the sensitivity of individual ECL systems without the nanomachine (4.97 fM) and individual walking nanomachine (340 fM) by 2 and 4 orders of magnitude, respectively, outperforming previous pathogenic bacteria analyses. The proposed ECL detection system exhibited an impressively low LOD of 9.0 CFU mL^{-1} for detecting *B. pseudomallei* in serum samples. In testing five serum samples spiked with *B. pseudomallei*, the ECL intensity showed relative standard deviations (RSD) ranging from 0.21% to 4.02%, underlining the precision of the biosensor. The ECL biosensor also demonstrated excellent recovery rates of 93.63–107.83% for detecting *B. pseudomallei* DNA-spiked serum samples.

Chen and co-authors applied nitrogen-doped graphene quantum dots (N-GQDs) to construct an ECL-based immunosensor for the detection of *E. coli* O157:H7 bacterium that produces Shiga toxins with polydopamine (PDA) surface imprinted polymer (SIP).[104] The synthesis of N-GQDs, possessing a high quantum yield of 43.2%, was achieved. A uniform PDA SIP film specific for *E. coli* O157:H7 was successfully created using a straightforward method. By directly electropolymerizing dopamine and the target bacterium on the electrode, the PDA SIP designed for *E. coli* O157:H7 was established effectively. Following the removal of the *E. coli* O157:H7 template, the developed PDA SIP exhibited selective recognition towards *E. coli* O157:H7. Subsequently, the *E. coli* O157:H7 polyclonal antibody (pAb) was labeled with N-GQDs. Combining the SIP-*E. coli* O157:H7/pAb-N-GQDs bioconjugation led to strong ECL emission under K$_2$S$_2$O$_8$, facilitating the detection of *E. coli* O157:H7 using the ECL system. This innovative approach demonstrated linear correlations between ECL intensity and *E. coli* O157:H7 concentration from 10^1 to 10^7 colony-forming units (CFU) mL^{-1}, with a detection limit of 8 CFU mL^{-1} when operating under optimized conditions. The biosensor utilizing this SIP film proved to be successful in detecting *E. coli* O157:H7 in water samples. A study performed by Zhou and coworkers presents ECL microscopy as a cutting-edge technology offering exceptional spatial and temporal resolution along with a distinctive chemical contrast for visualizing and distinguishing individual bacteria.[105] The method showcases precise bacterial quantification and classification accuracy of up to 90.5%. Additionally, they introduced an innovative tunable ECL imaging mode that transitions between negative contrast ECL imaging without labeling to positive contrast ECL imaging by leveraging [Ru(bpy)$_3$]$^{2+}$ for bacterial visualization. This flexibility enables detailed observation of a single bacterium at the molecular level.

In a study by Wang and co-authors a specialized ECL sensor was developed for both detecting and sterilization *Staphylococcus aureus*.[106] The sensor utilized silver nanoclusters labeled hairpin DNA (H-Ag NCs) as the energy acceptor responsible for receiving ECL emission from CdS quantum dots (CdS QDs), facilitating resonance energy transfer and ECL signal quenching. The ECL signal was amplified through energy transfer from ECL-excited surface plasmon resonance in Au NPs to CdS QDs. This innovative approach displayed effective *S. aureus* detection over a linear range of 5–108 CFU mL^{-1}. Moreover, this sensor system demonstrated exceptional discriminatory ability and efficacy in eliminating *S. aureus* in food samples, underscoring its practical reliability and utility.

3.4. ECL biosensors for DNA analysis

ECL immunosensing can be combined with ECL genosensing to improve disease diagnostics. The biorecognition of oligonucleotides by ECL genosensors is a beneficial diagnostic approach because of the high specificity of base-pairing interaction between complementary sequences. The biological sensing element in genosensors is a DNA probe, whose sequence is complementary to the DNA sequence of the target. Due to the specificity of the DNA probe, ECL genosensors can detect DNA nucleotide moieties,[107–109] RNA[110,111] and micro-RNA[112–115] which makes them suitable for a wide range of applications going from clinical diagnostics to food safety and environmental monitoring.

The binding of target sequences on the surface carrying the DNA probe generates signals that are further amplified. In recent years, various isothermal gene amplification techniques have been widely used in genosensors to enhance the signal. Moreover, ECL geno- and immunosensing can be combined to improve disease diagnostics. For instance, Zhao *et al.*, coupled a system based on Au nanoclusters (AuNCs)/Au–MnO$_2$ nanoflowers resonant energy transfer (RET) with rolling circle amplification (RCA) for the detection of PSA and Let-7a microRNA, that are both biomarkers of prostate cancer.[116] MicroRNAs, small (19–23 nt) noncoding RNAs, are reliable biomarkers not only for cancers but also for inflammatory bowel disease, cardiovascular and cerebrovascular diseases. Au NCs were employed for ECL signal enhancement through the stabilization of 3,4-thiophene dicarboxylic acid (TDA)-modified electrode. A sandwich ECL immunosensor for signal "OFF" detection of PSA was obtained with methionine-Au NCs with intense near-infrared ECL emission as ECL donors and Au–MnO$_2$ nanoflowers with strong light absorption capability as acceptors (Fig. 6). In addition, Let-7a microRNA was targeted *via* RCA reaction to produce long DNA nanowires, which when labeled with alkaline phosphatase, catalysed the production of ascorbic acid. Accumulation of ascorbic acid *in situ* reduced MnO$_2$, which inhibited ECL quenching and provided a "ON" detection of Let-7a. Such a dual biomarker detection is proposed for early clinical tumor diagnosis.

Recent years witnessed great development of metal–organic frameworks (MOF)-based ECL immuno- and genosensors.[117–119] Although MOF composites have poor intrinsic conductivity and low water solubility, they have exceptional physicochemical features, such as large surface
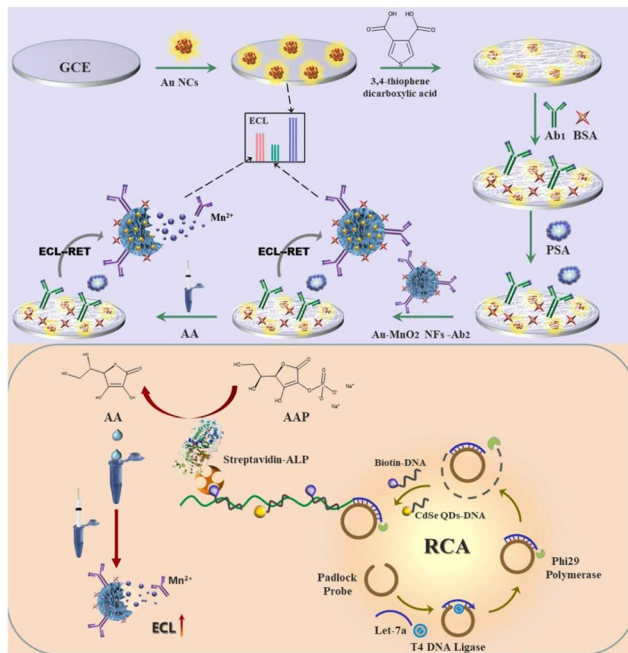
Fig. 6 Schematic of the ECL biosensor based on Au nanoclusters/Au–MnO₂ nanoflowers ECL-RET (resonant energy transfer) system coupled with RCA (rolling circle amplification) for dual target detection of PSA (prostate-specific antigen) and Let-7a microRNA.[116] Reprinted with permission from ref. 116 (copyright 2022 Elsevier).

area, high porosity, tunable size, tailorable structure and versatile functionality. To overcome their limitations, MOFs are combined with a variety of functional materials or loading guests such as ruthenium, luminol, and quantum dots. Alternatively, MOFs can be doped with transition metal elements to increase their low conductivity.[117,120] MOFs in ECL reactions for rapid detection of viral infection are of particular importance. Although viral infections can be detected by immunosensors, during the acute phase of infection specific antibodies are absent, and also immunosensors are unable to discriminate between current and previous infections. In contrast, direct detection of specific viral genes allows for early diagnosis. For instance, a 2D MOF with an excellent ECL performance was obtained by combining a porphyrin-based heterobimetallic MOF and a photosensitizer Zn^{2+}-tetrakis(4-carboxyphenyl)porphine (ZnTCPP) linker with the electroactive Co^{2+}-ions in the presence of 2-methylimidazole (MeIm).[121] The ECL sensor detected a low amount of the RdRp gene of SARS-CoV-2 (30 aM) without a need for target gene amplification. Finally, a new era of ECL biosensors for precise DNA analysis based on CRISPR (clustered regularly interspaced short palindromic repeats)–Cas systems are paving the way for the design of advanced diagnostics of infectious diseases, early-stage cancers, detrimental genetic conditions, and mutagenic defects.[122–125] Although CRISPR–Cas-based biosensors (especially using CRISPR-12a and CRIPR-13a systems for gene editing) are highly specific, fast, easy to use, and of low cost, they still have some drawbacks including the need for DNA amplification, and low reproducibility.

3.5. Cell analysis

Cancer cells are one of the greatest causes of death in human beings. ECL has been used to be the sensitive method for cancer cell detection. NPs, such as CdS NPs,[126–128] Au NPs,[129–131] are often utilized to construct the base of the ECL immunosensor for cell-level detection. CdS-coated-ZnO nanorod arrays labeled with 3-aminopropyltriethoxysilane and Au NPs, can not only offer the substrates for the conjugation of antibodies but also effectively enhance the ECL signal, resulting in the production of the high-performance ECL immunosensor. This immunosensor exhibits a sensitive response to HepG2 cells with a detection limit of 256 cells per mL.[126] Ding et al.[128] reported that CdS NPs were used to be functionalized with Au NPs and aptamer for electrochemical signal amplification, demonstrating excellent sensitivity and selectivity of the Ramos cells. Due to the unique amplification of Au NPs and the excellent selectivity of aptamers, the Ramos cells were rapidly and simply detected with high sensitivity. Later, Ding et al.[129] studied a polymerase chain reaction (PCR)-free ECL approach to determine cancer cells with high sensitivity based on aptamers, nanoparticles and magnetic beads. ECL probes consist of Au NPs with $[Ru(bpy)_3]^{2+}$, hybridize with the captured DNA with a magnetic bead to form the magnetic nanocomposite, which directly reflects the amount of cancer cells. Au nanostars (AuNSs) decorated with graphitic carbon nitride nanosheets (g-CN nanosheets) were designed to detect the CD133 peptide as a cancer stem cell membrane biomarker. AuNSs can increase electron transfer and electroreduced $S_2O_8^{2-}$, effectively enhancing the ECL intensity. Due to the localized surface plasmon resonance (LSPR) effect of AuNSs, AuNSs@g-CN nanosheets exhibited strong and stable cathodic ECL emission, realizing the detection of CD133 peptide in low concentration.[130]

4. Conclusions and perspectives

ECL has become a powerful technique for the ultrasensitive detection of a wide range of analytes, due to its inherent sensitivity, simplicity, well-control, and low background. Herein, we summarized the recent advances that have been made in novel ECL immunoassays, the ECL enhanced strategies, and the applications for the detection of biomarkers, DNA analysis, bacteria and cell analysis. These important topics cover the vast majority of the hotspots in the realm of ECL immunosensing. Clearly, the necessity of developing sensitive immunoassays and understanding fundamental ECL mechanisms have constantly stimulated breakthroughs in medical diagnosis, biological detection and tracking. Particular emphasis is placed on developing bead-based ECL immunoassays by using microscopy that aims to understand the mechanism of ECL of bead-based assays, to further assess at the single molecule level in the future, which could expand to other ECL sensing systems and ECL-based imaging. The commercialized ECL immunoassays are mainly based on the classical ECL system–ruthenium

complexes and TPrA. Meanwhile, other materials, such as Au nanomaterials, metal composites, carbon nanomaterials, or organic materials are often introduced into the ECL system to obtain stable and enhanced emission, improving efficiency. Fortunately, some novel immunosensing with new kinds of ECL materials and luminophores may promote the development of ECL technology.

Although novel ECL systems are overwhelmingly used to fabricate sensors with high efficiency, there are still great challenges as well as great opportunities to be faced in the future. First, though various signal amplification strategies have been designed, novel efficient ECL methodologies still need to be developed to understand the details of ECL kinetics and mechanisms, in order to meet the need for different applications. Second, despite the commercial immunosensing of $[Ru(bpy)_3]^{2+}$/TPrA system being successfully used, the high toxicity and poor biocompatibility of this system is still a major issue. Thus, more biocompatible and environmentally friendly ECL materials as the alternatives are highly desirable. Third, ECL emission can be observed at high positive or negative voltages, the problem is that the high voltage process unavoidably brings a series of undesired side effects, such as electrical damage to biological samples and hydrogen/oxygen evolution reactions. Therefore, it is urgently required to design and explore the low voltage-driven ECL luminophores,[132,133] not only to mitigate the electrode passivation but also to decrease the possibility of ECL change, which results from various physiological activities. Finally, the development of ECL-based point of care (POC) diagnostic devices, possibly with mobile phone powering and detection, constitutes a major direction in the field but it requires achieving full portability, de-laboratory, de-specialization and automation as detailed by several authors.[134–136]

In conclusion, we believe that ECL can have a brilliant future and fast development due to the great contributions from many researchers, and the affordable, sensitive, specific, user-friendly, rapid and robust, equipment-free ECL technology.

Data availability

The authors confirm that the data presented in this review are available within the cited articles.

Author contributions

N. S. defined the scope and J. Y. defined the structure of the review article. All the authors prepared the manuscript by writing the initial draft, drawing or selecting the illustrations, reviewing and editing.

Conflicts of interest

There are no conflicts to declare.

Acknowledgements

Notes and references

1 Z. Liu, W. Qi and G. Xu, *Chem. Soc. Rev.*, 2015, **44**, 3117–3142.
2 X. Ma, W. Gao, F. Du, F. Yuan, J. Yu, Y. Guan, N. Sojic and G. Xu, *Acc. Chem. Res.*, 2021, **54**, 2936–2945.
3 C. Ma, Y. Cao, X. Gou and J. J. Zhu, *Anal. Chem.*, 2020, **92**, 431–454.
4 M. Sornambigai, L. Bouffier, N. Sojic and S. S. Kumar, *Anal. Bioanal. Chem.*, 2023, **415**, 5875–5898.
5 K. D. Legg and D. M. Hercules, *J. Am. Chem. Soc.*, 1968, **91**, 1902–1907.
6 L. R. Faulkner and A. J. Bard, *J. Am. Chem. Soc.*, 1968, **90**, 6284–6290.
7 S. Knezevic, D. Han, B. Liu, D. Jiang and N. Sojic, *Angew. Chem., Int. Ed.*, 2024, **63**, e202407588.
8 S. Rebeccani, A. Zanut, C. I. Santo, G. Valenti and F. Paolucci, *Anal. Chem.*, 2022, **94**, 336–348.
9 Y. Liu, H. Zhang, B. Li, J. Liu, D. Jiang, B. Liu and N. Sojic, *J. Am. Chem. Soc.*, 2021, **143**, 17910–17914.
10 H. Qi and C. Zhang, *Anal. Chem.*, 2020, **92**, 524–534.
11 G. Liang, S. Liu, G. Zou and X. Zhang, *Anal. Chem.*, 2012, **84**, 10645–10649.
12 P. Zhou, S. Hu, W. Guo and B. Su, *Fundam. Res.*, 2022, **2**, 682–687.
13 N. Hao and K. Wang, *Anal. Bioanal. Chem.*, 2016, **408**, 7035–7048.
14 Z. Wang, J. Pan, Q. Li, Y. Zhou, S. Yang, J. J. Xu and D. Hua, *Adv. Funct. Mater.*, 2020, **30**, 2000220.
15 Z. Cao, Y. Shu, H. Qin, B. Su and X. Peng, *ACS Cent. Sci.*, 2020, **6**, 1129–1137.
16 E. Faatz, A. Finke, H. P. Josel, G. Prencipe, S. Quint and M. Windfuhr, *Analytical Electrogenerated Chemiluminescence*, 2019, pp. 443–469, DOI: 10.1039/9781788015776-fp001.
17 X. Gou, Z. Xing, C. Ma and J. J. Zhu, *Chem. Biomed. Imaging*, 2023, **1**, 414–433.
18 C. Mariani, S. Bogialli, F. Paolucci, P. Pastore, A. Zanut and G. Valenti, *Electrochim. Acta*, 2024, **489**, 144256.
19 H. Cui, W. Wang, C. F. Duan, Y. P. Dong and J. Z. Guo, *Chem. – Eur. J.*, 2007, **13**, 6975–6984.
20 A. Zanut, A. Fiorani, S. Canola, T. Saito, N. Ziebart, S. Rapino, S. Rebeccani, A. Barbon, T. Irie, H. P. Josel, F.

Negri, M. Marcaccio, M. Windfuhr, K. Imai, G. Valenti and F. Paolucci, *Nat. Commun.*, 2020, **11**, 2668.

21 M. Mayer, S. Takegami, M. Neumeier, S. Rink, A. Jacobi von Wangelin, S. Schulte, M. Vollmer, A. G. Griesbeck, A. Duerkop and A. J. Baeumner, *Angew. Chem., Int. Ed.*, 2018, **57**, 408–411.

22 P. Bertoncello, A. J. Stewart and L. Dennany, *Anal. Bioanal. Chem.*, 2014, **406**, 5573–5587.

23 A. Barhoum, Z. Altintas, K. S. S. Devi and R. J. Forster, *Nano Today*, 2023, **50**, 101874.

24 G. Valenti, E. Rampazzo, S. Kesarkar, D. Genovese, A. Fiorani, A. Zanut, F. Palomba, M. Marcaccio, F. Paolucci and L. Prodi, *Coord. Chem. Rev.*, 2018, **367**, 65–81.

25 A. Zanut, F. Palomba, M. Rossi Scota, S. Rebeccani, M. Marcaccio, D. Genovese, E. Rampazzo, G. Valenti, F. Paolucci and L. Prodi, *Angew. Chem., Int. Ed.*, 2020, **59**, 21858–21863.

26 G. Valenti, E. Rampazzo, S. Bonacchi, L. Petrizza, M. Marcaccio, M. Montalti, L. Prodi and F. Paolucci, *J. Am. Chem. Soc.*, 2016, **138**, 15935–15942.

27 E. R. Simone Zanarini, S. Bonacchi, R. Juris, M. Marcaccio, M. Montalti, F. Paolucci and L. Prodi, *J. Am. Chem. Soc.*, 2009, **131**, 14208–14209.

28 Z. Ding, B. M. Quinn, S. K. Haram, L. E. Pell, B. A. Korgel and A. J. Bard, *Science*, 2002, **296**, 1293–1297.

29 T. Zhao, Q. Zhou, Y. Lv, D. Han, K. Wu, L. Zhao, Y. Shen, S. Liu and Y. Zhang, *Angew. Chem., Int. Ed.*, 2020, **59**, 1139–1143.

30 E. Yang, Y. Zhang and Y. Shen, *Anal. Chim. Acta*, 2022, **1209**, 339140.

31 M. Hesari and Z. Ding, *J. Am. Chem. Soc.*, 2021, **143**, 19474–19485.

32 M. Hesari, M. S. Workentin and Z. Ding, *ACS Nano*, 2014, **8**, 8543–8553.

33 J. M. Kim, S. Jeong, J. K. Song and J. Kim, *Chem. Commun.*, 2018, **54**, 2838–2841.

34 Y. Kang and J. Kim, *ChemElectroChem*, 2020, **7**, 1092–1096.

35 Z. Huang, Z. Li, Y. Chen, L. Xu, Q. Xie, H. Deng, W. Chen and H. Peng, *Anal. Chem.*, 2021, **93**, 4635–4640.

36 D. Wang, X. Gao, J. Jia, B. Zhang and G. Zou, *ACS Nano*, 2023, **17**, 355–362.

37 P. Sabhachandani, S. Sarkar, P. C. Zucchi, B. A. Whitfield, J. E. Kirby, E. B. Hirsch and T. Konry, *Microchim. Acta*, 2017, **184**, 4619–4628.

38 N. Scholler, M. Crawford, A. Sato, C. W. Drescher, K. C. O'Briant, N. Kiviat, G. L. Anderson and N. Urban, *Clin. Cancer Res.*, 2006, **12**, 2117–2124.

39 K. Y. Lien, L. Y. Hung, T. B. Huang, Y. C. Tsai, H. Y. Lei and G. B. Lee, *Biosens. Bioelectron.*, 2011, **26**, 3900–3907.

40 M. Sentic, M. Milutinovic, F. Kanoufi, D. Manojlovic, S. Arbault and N. Sojic, *Chem. Sci.*, 2014, **5**, 2568–2572.

41 Y. Feng, W. Zhou, X. Wang, J. Zhang, M. Zou, C. Zhang and H. Qi, *Chem. Biomed. Imaging*, 2023, **1**, 648–658.

42 D. Han, D. Fang, G. Valenti, F. Paolucci, F. Kanoufi, D. Jiang and N. Sojic, *Anal. Chem.*, 2023, **95**, 15700–15706.

43 A. Fracassa, C. I. Santo, E. Kerr, S. Knezevic, D. J. Hayne, P. S. Francis, F. Kanoufi, N. Sojic, F. Paolucci and G. Valenti, *Chem. Sci.*, 2024, **15**, 1150–1158.

44 D. Han, D. Jiang, G. Valenti, F. Paolucci, F. Kanoufi, P. C. Chaumet, D. Fang and N. Sojic, *ACS Sens.*, 2023, **8**, 4782–4791.

45 Y. Wang, J. Ding, P. Zhou, J. Liu, Z. Qiao, K. Yu, J. Jiang and B. Su, *Angew. Chem., Int. Ed.*, 2023, **62**, e202216525.

46 L. Xiao, Y. Chai, R. Yuan, Y. Cao, H. Wang and L. Bai, *Talanta*, 2013, **115**, 577–582.

47 S. Rebeccani, C. Wetzl, V. A. Zamolo, A. Criado, G. Valenti, F. Paolucci and M. Prato, *Chem. Commun.*, 2021, **57**, 9672–9675.

48 X. Yang, J. Hang, W. Qu, Y. Wang, L. Wang, P. Zhou, H. Ding, B. Su, J. Lei, W. Guo and Z. Dai, *J. Am. Chem. Soc.*, 2023, **145**, 16026–16036.

49 M. Sentic, F. Virgilio, A. Zanut, D. Manojlovic, S. Arbault, M. Tormen, N. Sojic and P. Ugo, *Anal. Bioanal. Chem.*, 2016, **408**, 7085–7094.

50 H. B. Habtamu, M. Sentic, M. Silvestrini, L. De Leo, T. Not, S. Arbault, D. Manojlovic, N. Sojic and P. Ugo, *Anal. Chem.*, 2015, **87**, 12080–12087.

51 X. Yang, Y. Wei, Y. Du, H. Qi, Q. Gao and C. Zhang, *Anal. Chem.*, 2020, **92**, 15837–15844.

52 G. Valenti, A. Fiorani, H. Li, N. Sojic and F. Paolucci, *ChemElectroChem*, 2016, **3**, 1990–1997.

53 X. Yang, Y. Xu, X. Huang, J. Hang, W. Guo and Z. Dai, *Anal. Chem.*, 2023, **95**, 4543–4549.

54 W. Guo, H. Ding, C. Gu, Y. Liu, X. Jiang, B. Su and Y. Shao, *J. Am. Chem. Soc.*, 2018, **140**, 15904–15915.

55 J. M. Fernandez-Hernandez, E. Longhi, R. Cysewski, F. Polo, H. P. Josel and L. De Cola, *Anal. Chem.*, 2016, **88**, 4174–4178.

56 M. A. Haghighatbin, S. E. Laird and C. F. Hogan, *Curr. Opin. Electrochem.*, 2018, **7**, 216–223.

57 K. Sakanoue, A. Fiorani, C. I. Santo, Irkham, G. Valenti, F. Paolucci and Y. Einaga, *ACS Sens.*, 2022, **7**, 1145–1155.

58 A. Fiorani, C. I. Santo, K. Sakanoue, D. Calabria, M. Mirasoli, F. Paolucci, G. Valenti and Y. Einaga, *Anal. Bioanal. Chem.*, 2024, DOI: **10.1007/s00216-024-05356-z**.

59 B. M. B. Factor, S. Workman, E. Bolton, J. Bos and M. M. Richter, *Anal. Chem.*, 2001, **73**, 4621–4624.

60 S. Kirschbaum-Harriman, A. Duerkop and A. J. Baeumner, *Analyst*, 2017, **142**, 2648–2653.

61 A. Fiorani, D. Han, D. Jiang, D. Fang, F. Paolucci, N. Sojic and G. Valenti, *Chem. Sci.*, 2020, **11**, 10496–10500.

62 P. Dutta, D. Han, B. Goudeau, D. Jiang, D. Fang and N. Sojic, *Biosens. Bioelectron.*, 2020, **165**, 112372.

63 E. Kerr, S. Knezevic, P. S. Francis, C. F. Hogan, G. Valenti, F. Paolucci, F. Kanoufi and N. Sojic, *ACS Sens.*, 2023, **8**, 933–939.

64 S. J. Blom, N. S. Adamson, E. Kerr, E. H. Doeven, O. S. Wenger, R. S. Schaer, D. J. Hayne, F. Paolucci, N. Sojic, G. Valenti and P. S. Francis, *Electrochim. Acta*, 2024, **484**, 143957.

65 S. B. N. Adamson, E. Doeven, T. Connell, C. Hadden, S. Knežević, N. Sojic, A. Fracassa, G. Valenti, F. Paolucci, J.

Ding, Y. Wang, B. Su, C. Hua and P. Francis, *Angew. Chem., Int. Ed.*, 2024, **63**, e202412097.

66 D. Han, B. Goudeau, V. Lapeyre, V. Ravaine, D. Jiang, D. Fang and N. Sojic, *Biosens. Bioelectron.*, 2022, **216**, 114640.

67 J. Dong, Y. Lu, Y. Xu, F. Chen, J. Yang, Y. Chen and J. Feng, *Nature*, 2021, **596**, 244–249.

68 W. Zhu, J. Dong, G. Ruan, Y. Zhou and J. Feng, *Angew. Chem., Int. Ed.*, 2023, **62**, e202214419.

69 F. Du, Y. Chen, C. Meng, B. Lou, W. Zhang and G. Xu, *Curr. Opin. Electrochem.*, 2021, **28**, 100725.

70 M. Guo, D. Du, J. Wang, Y. Ma, D. Yang, M. A. Haghighatbin, J. Shu, W. Nie, R. Zhang, Z. Bian, L. Wang, Z. J. Smith and H. Cui, *Chem. Biomed. Imaging*, 2023, **1**, 179–185.

71 W. Fu, X. Wang, X. Ying, T. Sun, Y. Wang, J. Wang and B. Su, *Adv. Funct. Mater.*, 2024, 2409632, DOI: **10.1002/adfm.202409632**.

72 C. Y. Huang, F. Y. Lin, C. J. Chang, C. H. Lu and J. K. Chen, *Anal. Chem.*, 2023, **95**, 986–993.

73 S. Yuan, R. Yuan, Y. Chai, L. Mao, X. Yang, Y. Yuan and H. Niu, *Talanta*, 2010, **82**, 1468–1471.

74 X. Dong, G. Zhao, Y. Li, Q. Zeng, H. Ma, D. Wu, X. Ren, Q. Wei and H. Ju, *Anal. Chem.*, 2022, **94**, 12742–12749.

75 J. Li, H. Yang, R. Cai and W. Tan, *ACS Appl. Mater. Interfaces*, 2022, **14**, 44222–44227.

76 X. Zheng, G. Mo, Y. He, D. Qin, X. Jiang, W. Mo and B. Deng, *J. Electroanal. Chem.*, 2019, **844**, 132–141.

77 Y. Hu, Y. Chen, Q. Tang and H. Liu, *New J. Chem.*, 2021, **45**, 12613–12621.

78 M. Li, M. Zhang, S. Ge, M. Yan, J. Yu, J. Huang and S. Liu, *Sens. Actuators, B*, 2013, **181**, 50–56.

79 X. Li, Y. Xu and L. Zhang, *Prog. Mol. Biol. Transl. Sci.*, 2019, **162**, 265–276.

80 H. W. Shi, W. Zhao, Z. Liu, X. C. Liu, M. S. Wu, J. J. Xu and H. Y. Chen, *Talanta*, 2016, **154**, 169–174.

81 L. Fu, K. Fu, X. Gao, S. Dong, B. Zhang, S. Fu, H. Y. Hsu and G. Zou, *Anal. Chem.*, 2021, **93**, 2160–2165.

82 J. T. Cao, X. M. Liu, Y. Z. Fu, S. W. Ren and Y. M. Liu, *Anal. Lett.*, 2022, **55**, 1810–1821.

83 F. Li, Y. Yu, H. Cui, D. Yang and Z. Bian, *Analyst*, 2013, **138**, 1844–1850.

84 F. Du, Z. Dong, Y. Guan, A. M. Zeid, D. Ma, J. Feng, D. Yang and G. Xu, *Anal. Chem.*, 2022, **94**, 2189–2194.

85 D. Hong, K. Kim, E. J. Jo and M. G. Kim, *Anal. Chem.*, 2021, **93**, 7925–7932.

86 R. Zhou, C. Fang, J. Yan and Y. Tu, *Talanta*, 2019, **205**, 120135.

87 H. Qin, X. Gao, X. Yang, W. Cao and S. Liu, *Biosens. Bioelectron.*, 2019, **141**, 111438.

88 R. Tan, Y. Wang, X. Mi, H. Li and Y. Tu, *Sens. Actuators, B*, 2022, **352**, 131065.

89 D. Fang, M. Pan, H. Yi, H. Dai, Z. Hong, X. Zheng and Y. Lin, *Sens. Actuators, B*, 2019, **286**, 608–615.

90 D. Fang, S. Zhang, H. Dai and Y. Lin, *Biosens. Bioelectron.*, 2019, **146**, 111768.

91 Y. Z. X. Liu, J. Lei, Y. Xue, L. Cheng and H. Ju, *Anal. Chem.*, 2010, **82**, 7351–7356.

92 G. Jie, P. Liu, L. Wang and S. Zhang, *Electrochem. Commun.*, 2010, **12**, 22–26.

93 J. Liu, X. Liu, H. Chen, L. Yang, A. Cai, H. Ji, Q. Wang, X. Zhou, G. Li, M. Wu, Y. Qin and L. Wu, *Anal. Chem.*, 2022, **94**, 7115–7122.

94 Y. Du, X. Li, X. Ren, H. Wang, D. Wu, H. Ma, D. Fan and Q. Wei, *Analyst*, 2020, **145**, 1858–1864.

95 Y. Liu, Q. Zhang, H. Wang, Y. Yuan, Y. Chai and R. Yuan, *Biosens. Bioelectron.*, 2015, **71**, 164–170.

96 X. Shao, X. Song, X. Liu, L. Yan, L. Liu, D. Fan, Q. Wei and H. Ju, *Microchim. Acta*, 2021, **188**, 344.

97 N. Liao, Y. Zhuo, Y. Chai, Y. Xiang, Y. Cao, R. Yuan and J. Han, *Chem. Commun.*, 2012, **48**, 7610–7612.

98 Y. Q. Yu, H. Y. Zhang, Y. Q. Chai, R. Yuan and Y. Zhuo, *Biosens. Bioelectron.*, 2016, **85**, 8–15.

99 G. Y. Zhang, C. Cai, S. Cosnier, H. B. Zeng, X. J. Zhang and D. Shan, *Nanoscale*, 2016, **8**, 11649–11657.

100 H. Wang, Y. Yuan, Y. Zhuo, Y. Chai and R. Yuan, *Anal. Chem.*, 2016, **88**, 2258–2265.

101 Y. Zhuo, N. Liao, Y. Q. Chai, G. F. Gui, M. Zhao, J. Han, Y. Xiang and R. Yuan, *Anal. Chem.*, 2014, **86**, 1053–1060.

102 W. Wei, H. Lin, T. Hao, X. Su, X. Jiang, S. Wang, Y. Hu and Z. Guo, *Sens. Actuators, B*, 2021, **332**, 129525.

103 Y. Wang, R. Chen, B. Shen, C. Li, J. Chen, Y. Wang, S. Tian, X. Li, N. Luo, R. Liu, S. Ding, C. Zhu and Q. Xia, *Microchim. Acta*, 2022, **189**, 355.

104 S. Chen, X. Chen, L. Zhang, J. Gao and Q. Ma, *ACS Appl. Mater. Interfaces*, 2017, **9**, 5430–5436.

105 Y. Zhou, J. Dong, P. Zhao, J. Zhang, M. Zheng and J. Feng, *J. Am. Chem. Soc.*, 2023, **145**, 8947–8953.

106 C. Wang, T. Wu, X. Miao, P. Wang and Q. Feng, *Talanta*, 2023, **253**, 124074.

107 Y. Chen, J. Xu, J. Su, Y. Xiang, R. Yuan and Y. Chai, *Anal. Chem.*, 2012, **84**, 7750–7755.

108 P. F. Liu, K. R. Zhao, Z. J. Liu, L. Wang, S. Y. Ye and G. X. Liang, *Biosens. Bioelectron.*, 2021, **176**, 112954.

109 Y. Liu, Y. Wei, Y. Cao, D. Zhu, W. Ma, Y. Yu and M. Guo, *Biosens. Bioelectron.*, 2018, **117**, 830–837.

110 L. Gutierrez-Galvez, R. Del Cano, I. Menendez-Luque, D. Garcia-Nieto, M. Rodriguez-Pena, M. Luna, T. Pineda, F. Pariente, T. Garcia-Mendiola and E. Lorenzo, *Talanta*, 2022, **240**, 123203.

111 Y. W. Zhang, W. S. Liu, J. S. Chen, H. L. Niu, C. J. Mao and B. K. Jin, *Sens. Actuators, B*, 2020, **321**, 128456.

112 J. Zhao, J. Luo, D. Liu, Y. He, Q. Li, S. Chen and R. Yuan, *Sens. Actuators, B*, 2020, **316**, 128139.

113 X. Meng, X. Pang, J. Yang, X. Zhang and H. Dong, *Small*, 2024, **20**, e2307701.

114 Z. Ning, E. Yang, Y. Zheng, M. Chen, G. Wu, Y. Zhang and Y. Shen, *Anal. Chem.*, 2021, **93**, 8971–8977.

115 J. M. Wang, L. Y. Yao, W. Huang, Y. Yang, W. B. Liang, R. Yuan and D. R. Xiao, *ACS Appl. Mater. Interfaces*, 2021, **13**, 44079–44085.

116 Y. Zhao, R. Wang, Y. Xue and G. Jie, *Sens. Actuators, B*, 2022, **369**, 132397.

117 M. Sentic, I. Trajkovic, D. Manojlovic, D. Stankovic, M. V. Nikolic, N. Sojic and J. Vidic, *Materials*, 2023, **16**, 7502.

118 J. Zhou, Y. Li, W. Wang, X. Tan, Z. Lu and H. Han, *Biosens. Bioelectron.*, 2020, **164**, 112332.

119 W. Li, Z. Liang, P. Wang and Q. Ma, *Biosens. Bioelectron.*, 2024, **249**, 116008.

120 H. Fu, Z. Xu, H. Hou, R. Luo, H. Ju and J. Lei, *Chemosensors*, 2023, **11**, 422.

121 Y. X. Li, J. Li, D. Zhu, J. Z. Wang, G. F. Shu, J. Li, S. L. Zhang, X. J. Zhang, S. Cosnier, H. B. Zeng and D. Shan, *Adv. Funct. Mater.*, 2022, 202209743, DOI: **10.1002/adfm.202209743**.

122 L. Mei-Ling, L. Yi, Z. Mei-Ling, Z. Ying and H. Xiao-Jing, *Biosens. Bioelectron.*, 2022, **214**, 114512.

123 Z. H. Xu, Z. Y. Zhao, H. Wang, S. M. Wang, H. Y. Chen and J. J. Xu, *Anal. Chim. Acta*, 2021, **1188**, 339180.

124 K. Zhang, Z. Fan, B. Yao, Y. Ding, J. Zhao, M. Xie and J. Pan, *Biosens. Bioelectron.*, 2021, **178**, 113019.

125 S. Y. L. Li, J. Wu and H. Ju, *Anal. Chem.*, 2013, **95**, 7396–7402.

126 D. Liu, L. Wang, S. Ma, Z. Jiang, B. Yang, X. Han and S. Liu, *Nanoscale*, 2015, **7**, 3627–3633.

127 E. Han, L. Ding, S. Jin and H. Ju, *Biosens. Bioelectron.*, 2011, **26**, 2500–2505.

128 C. Ding, Y. Ge and S. Zhang, *Chem*, 2010, **16**, 10707–10714.

129 C. Ding, S. Wei and H. Liu, *Chem*, 2012, **18**, 7263–7268.

130 S. Chenaghlou, A. Khataee, R. Jalili, M. R. Rashidi, B. Khalilzadeh and S. Woo Joo, *Bioelectrochemistry*, 2021, **137**, 107633.

131 A. Zhang, W. Guo, H. Ke, X. Zhang, H. Zhang, C. Huang, D. Yang, N. Jia and D. Cui, *Biosens. Bioelectron.*, 2018, **101**, 219–226.

132 Y. Ju, H. J. Park, I. S. Shin, Y. K. Chung and J. Kim, *Inorg. Chem. Commun.*, 2019, **106**, 86–90.

133 Y. Z. Wang, Y. R. Li, Y. Q. Zhang, Y. M. Xiang, R. R. Bai, Y. Liu, M. L. Li, G. R. Meng, S. L. Pan, F. Zhang, L. Mi and Y. H. Hu, *Biosens. Bioelectron.*, 2024, **261**, 116495.

134 M. Jović, D. Prim, O. Righini, D. Tagan, M. Stäuble, M. Pignat, S. Gallay, M. Geiser and M. E. Pfeifer, *Sens. Diagn.*, 2023, **2**, 964–975.

135 X. Ying, L. Zhou, W. Fu, Y. Wang and B. Su, *Sens. Diagn.*, 2023, **2**, 480–491.

136 J. Totoricaguena-Gorrino, M. Dei, A. F. Alba, N. Perinka, L. R. Rubio, J. L. Vilas-Vilela and F. J. Del Campo, *ACS Sens.*, 2022, **7**, 1544–1554.